A Quantitative Study on Optimum Parameters Selection in Adaptive Unsharp Masking Technique for Infrared Images

Onur JANE, H. Gökhan İLK

Ankara University, Faculty of Engineering, Electronics Engineering Dept., Ankara, Turkey

onur_jane@yahoo.co.uk, ilk@ieee.org

Abstract. *Infrared image processing has been the focal point of considerable research activity in the last decade mainly because of its wide application areas in security and defense. With the aid of an existing image enhancement technique, we propose an optimum parameters selection procedure which delivers better performance in sharpness and contrast adjustment for the detection of targets in interest in objective quality metrics. Hence, proposed method ensures that the edges of the targets in infrared images are sharper and that the quality of contrast adjustment has its optimum level with minimum error.*

Keywords

Adaptive filtering, surveillance applications, image enhancement, Gauss-Newton algorithm, minimum mean square error.

1. Introduction

Infrared imaging has its roots in surveillance and crime deterrence for approximately half a century [1]. Since then, besides infrared imaging, both image and infrared image processing algorithms have found many applications. Especially military applications such as occupation detection, bomber defense, area surveillance, terrain analysis, and detection of personnel, vehicles and weapons are provided by infrared devices [2]. The application areas are so vast that scenarios including damage assessment, automatic target detection and tracking for sea surface targets have also been studied in the literature [3].

The Classic Linear Unsharp Masking (CLUM) technique improves high frequency components of an image for a better view. That's why this technique is frequently used for sharpening, enhancing the edge components and adjusting the contrast levels of the image. As shown in Fig. 1 [4], with the CLUM technique, the input image $x(n,m)$ is firstly driven to a linear high pass filter, then the high pass filter output image $z(n,m)$ is scaled with an appropriate coefficient λ. Finally, scaled image is added to the input image to obtain the output image $y(n,m)$.

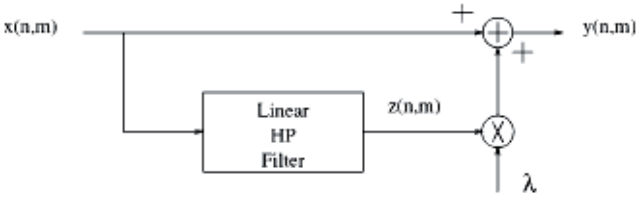

Fig. 1. The block diagram of the CLUM technique.

Although the CLUM technique with its simple structure is useful in many applications, two drawbacks of that technique should be taken into consideration:

First drawback is that the CLUM technique makes the system sensitive to noise, which means it leads unwanted distortion in the uniform areas on images [5]. Second and final drawback is that the CLUM technique enhances the areas with high contrast level much more than the areas with low and medium contrast levels. Eventually, the resulting image is observed extremely artificial [5].

Noise amplification and extreme artificiality problems observed in the CLUM technique can be prevented by using the "Adaptive Unsharp Masking (AUM)" technique. On the contrary of the CLUM technique, the AUM technique updates the coefficients recursively by using some parameters and adaptive algorithm so that for the areas with low contrast level (uniform areas), there is no sharpening path or no enhancement; for the areas with medium contrast level, there is an enhancement close to the moderation for the areas with high contrast levels which are partially enhanced.

In this study, AUM, the image enhancement technique which was initially proposed for visible band in [4], is used to improve the quality of infrared images that are obtained from the heat distribution of targets in infrared band, so that enhanced images will be much more appropriate than the original one for the purpose of security and defense [6]. The rest of this paper includes the following sections. Section 2 gives the AUM technique in detail. Section 3 interprets the parameters and gives guidance to select optimum values for infrared images in this technique. In Section 4, the experimental results for the proposed procedures in Section 3 are presented. Section 5 finally concludes this work.

2. Adaptive Unsharp Masking Technique

As illustrated in Fig. 1 and explained in (1) [4], with the CLUM technique, the input image $x(n,m)$ is firstly driven to a linear high pass filter and the high pass filter output image $z(n,m)$ is scaled with an appropriate coefficient λ, then the scaled image is added to the input image.

$$y(n,m) = x(n,m) + \lambda z(n,m). \quad (1)$$

Hence, the optimum contrast level of the input image can be obtained. The differences between the CLUM and the AUM techniques are the selection of updated coefficients λ and the filter characteristics whose outputs are $z(n,m)$. In the CLUM technique, linear high pass filter output is shown in (2) [4].

$$z(n,m) = 4x(n,m) - x(n-1,m) - x(n+1,m) - x(n,m-1) - x(n,m+1). \quad (2)$$

In the AUM technique however, according to two directional Laplacian operator used, equation (2) is organized and broken into two parts as horizontal filter output in (3)

$$z_x(n,m) = 2x(n,m) - x(n,m-1) - x(n,m+1) \quad (3)$$

and as vertical filter output in (4) [4].

$$z_y(n,m) = 2x(n,m) - x(n-1,m) - x(n+1,m) \quad (4)$$

Thus, updated version of the CLUM technique in (1) is obtained for the AUM technique as given in (5) [4].

$$y(n,m) = x(n,m) + \lambda_x(n,m) z_x(n,m) + \lambda_y(n,m) z_y(n,m). \quad (5)$$

By defining the scaling vector $\boldsymbol{\Lambda}(n,m)$ in (6) [4]

$$\boldsymbol{\Lambda}(n,m) = \left[\lambda_x(n,m), \lambda_y(n,m)\right]^T \quad (6)$$

and the correction vector $\boldsymbol{Z}(n,m)$ in (7) [4],

$$\boldsymbol{Z}(n,m) = \left[z_x(n,m), z_y(n,m)\right]^T. \quad (7)$$

Equation (5) can be reorganized as in (8) [4].

$$y(n,m) = x(n,m) + \boldsymbol{\Lambda}^T(n,m)\boldsymbol{Z}(n,m). \quad (8)$$

The use of the scaling vectors in both horizontal and vertical axes is due to the sensitivity of human eye to different directions: anisotropic effect [7].

With this remedial technique and adaptive algorithm, the scaling vector updates itsself by using the feedback structure shown in Fig. 2 [4]. $y(n,m)$, the output of the block diagram in Fig. 2, is an image whose uniform areas don't change and which have local dynamic pixels improving the contrast level of detailed areas. As a result, two drawbacks mentioned in Section 1 can be avoided successfully.

To calculate local dynamic pixels, a 3X3-pixel high pass filter shown as the operator $g(.)$ in Fig. 3 [4] is used in order to be consistent with the results presented in [4]. In this case, represented local dynamic images are $g_x(n,m)$ for the input image $x(n,m)$, $g_{zx}(n,m)$ for the horizontal filter output $z_x(n,m)$ and $g_{zy}(n,m)$ for the vertical filter output $z_y(n,m)$.

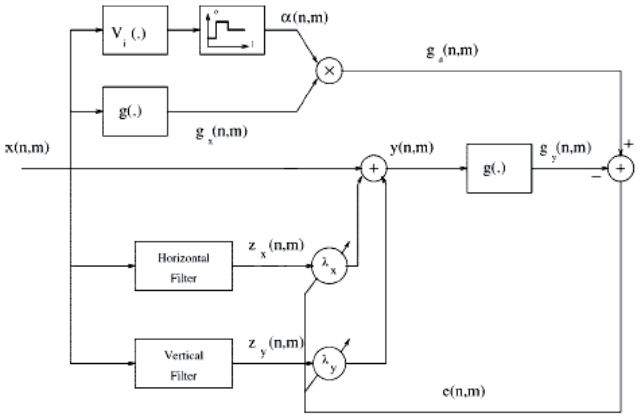

Fig. 2. The block diagram of the AUM technique.

-1	-1	-1
-1	8	-1
-1	-1	-1

Fig. 3. The operator $g(.)$.

The actual local dynamic image $g_y(n,m)$, which is derived from (8), is obtained by the use of adaptive filter as shown in (9) [4]:

$$g_y(n,m) = g_x(n,m) + g_{(\Lambda^T Z)}(n,m). \quad (9)$$

According to Fig. 2, desired local dynamic image $g_d(n,m)$ and actual local dynamic image $g_y(n,m)$ is expected to be similar. Therefore the key parameter, to minimize the error $e(n,m)$, is the scaling vector $\boldsymbol{\Lambda}(n,m)$ which is updated in every pixel with the adaptive algorithm. To implement this algorithm, firstly, mean value on 3X3 neighborhood of $(n,m)^{th}$ pixel of the input image $x(n,m)$ is calculated [4] as $\lfloor \bar{x}(n,m) \rfloor$. Then, local variance image $v_i(n,m)$ is obtained by using both the input image and its mean image as described in (10).

$$v_i(n,m) = \frac{1}{9} \sum_{i=n-1}^{n+1} \sum_{j=m-1}^{m+1} \left[x(i,j) - \bar{x}(n,m)\right]^2. \quad (10)$$

In terms of the input image $x(n,m)$, local variance image $v_i(n,m)$ for each pixel is compared to τ_1 and τ_2 thresholds having inequality condition as $\tau_1 < \tau_2$. According to the algorithm, the input image $x(n,m)$ is split into three different contrast areas in order to satisfy the following conditions: $v_i(n,m) < \tau_1$ for uniform or low contrast level areas, $\tau_1 \le v_i(n,m) < \tau_2$ for medium contrast level areas and $v_i(n,m) \ge \tau_2$ for high contrast level areas [4]. Thus, variable gain image $\alpha(n,m)$ in (11) is obtained by using the classifi-

cation based on the intensity levels of the variance image $v_i(n,m)$ [4].

$$\alpha(n,m)=\begin{cases}1, & v_i(n,m)<\tau_1\\ \alpha_{dh}(>1), & \tau_1\le v_i(n,m)<\tau_2\\ \alpha_{dl}(1<\alpha_{dl}<\alpha_{dh}), & v_i(n,m)\ge\tau_2\end{cases} \quad (11)$$

where α_{dh} and α_{dl} represent medium and high contrast level enhancement coefficients respectively.

Local dynamic image for the input image $g_x(n,m)$ is multiplied by variable gain image $\alpha(n,m)$ to find desired local dynamic image $g_d(n,m)$ in (12) [4].

$$g_d(n,m)=\alpha(n,m)g_x(n,m). \quad (12)$$

Moreover, actual local dynamic image can be calculated from (13)

$$g_y(n,m)=g_x(n,m)+\boldsymbol{\Lambda}^T(n,m)\boldsymbol{G}(n,m) \quad (13)$$

where $\boldsymbol{G}(n,m)$ is the input vector to adaptive filter as shown in (14) [4].

$$\boldsymbol{G}(n,m)=\left[g_{zx}(n,m),g_{zy}(n,m)\right]^T. \quad (14)$$

The output image $y(n,m)$ has the desired contrast level and is enhanced sharply by using the feedback structure [5] in Fig. 2. Thus, the algorithm which adjusts the contrast level of the original image to its desired enhanced level by updating the scaling vector and by minimizing the error at the same time is the Gauss-Newton algorithm [8]. By means of this algorithm, $\boldsymbol{\Lambda}(n,m)$ in (8) can now be calculated recursively in (15).

$$\begin{aligned}\boldsymbol{\Lambda}(n,m+1)&=\boldsymbol{\Lambda}(n,m)-\mu\boldsymbol{R}^{-1}(n,m)\frac{\partial}{\partial\boldsymbol{\Lambda}(n,m)}\left[e^2(n,m)\right]\\ &=\boldsymbol{\Lambda}(n,m)-2\mu e(n,m)\boldsymbol{R}^{-1}(n,m)\frac{\partial e(n,m)}{\partial\boldsymbol{\Lambda}(n,m)}\\ &=\boldsymbol{\Lambda}(n,m)-2\mu e(n,m)\boldsymbol{R}^{-1}(n,m)\frac{\partial\left[g_d(n,m)-g_y(n,m)\right]}{\partial\boldsymbol{\Lambda}(n,m)}\\ &=\boldsymbol{\Lambda}(n,m)-2\mu e(n,m)\boldsymbol{R}^{-1}(n,m)\frac{\partial\left[\alpha(n,m)g_x(n,m)\right]}{\partial\boldsymbol{\Lambda}(n,m)}\\ &\quad-2\mu e(n,m)\boldsymbol{R}^{-1}(n,m)\frac{\partial\left[g_x(n,m)-\boldsymbol{\Lambda}^T(n,m)\boldsymbol{G}(n,m)\right]}{\partial\boldsymbol{\Lambda}(n,m)}\\ &=\boldsymbol{\Lambda}(n,m)+2\mu e(n,m)\boldsymbol{R}^{-1}(n,m)\boldsymbol{G}(n,m)\end{aligned} \quad (15)$$

That is, the value of each column location in each row of the scaling vector is calculated by using the value of the same row of the previous column. Hence, for the scaling vector, the values of each row location in the first column have its initial values which are updated with the use of the feedback structure. μ in (15) is a parameter determining the convergence rate or speed of the adaptive filter.

Before applying the Gauss-Newton algorithm in (15), the input vector to adaptive filter $\boldsymbol{G}(n,m)$ in (14) is used to calculate its autocorrelation matrix recursively in (16) as the scaling vector is obtained [4].

$$\boldsymbol{R}(n,m)=(1-\beta)\boldsymbol{R}(n,m-1)+\beta\boldsymbol{G}(n,m)\boldsymbol{G}^T(n,m). \quad (16)$$

The value of each column location in each row of the autocorrelation matrix is obtained by using the value of the same row of the previous column. Hence, for the autocorrelation matrix, the values of each row location in the first column have its initial values which are updated recursively. β in (16) is a positive real number which is called convergence parameter and should be less than 1.

Consequently, the input image $x(n,m)$ is added to the correction vector $\boldsymbol{Z}(n,m)$ which is scaled by the updated correction vector $\boldsymbol{\Lambda}(n,m)$ as shown in (8). Therefore, contrast-adjusted and sharply enhanced output image $y(n,m)$ is obtained by the AUM technique. The next section will address the physical interpretation and selection of optimum value criterions for the parameters related to the AUM technique.

3. Parameter Interpretation and Selection of Optimum Values for Infrared Images in Adaptive Unsharp Masking

The adaptive unsharp masking algorithm described in [4] concentrates on contrast and sharpness level of the input image $x(n,m)$ and minimizes the error between desired and actual local dynamic images $g_d(n,m)$ and $g_y(n,m)$ respectively.

Although the algorithm might be seen trivial at first glance, it is well reported and cited in the literature extensively (more than 100 times) [9-13]. This important work however, lacks the interpretation of vital parameters and selection of optimum values in a clear and concise manner. The rest of this section will therefore elaborate these parameters listed in Tab. 1 and will examine the effects observed on the output image $y(n,m)$, desired local dynamic image $g_d(n,m)$, actual dynamic image $g_y(n,m)$, and the error image $e(n,m)$ for a sea surface infrared image.

Parameter	Explanations
τ_1	Lower limit threshold for medium contrast level areas
τ_2	Upper limit threshold for medium contrast level areas
α_{dl}	High contrast level enhancement coefficient
α_{dh}	Medium contrast level enhancement coefficient
μ	Convergence rate of adaptive filter
Λ	Scaling vector
β	Positive convergence parameter
R	Autocorrelation matrix of the input vector to adaptive filter G

Tab. 1. Required parameters for adaptive unsharp masking filter.

Polesel et al. report; since there is no reference image and conditions may be different for the observers to decide whether the output image $y(n,m)$ is good enough, it is better to determine the quality of the output image by using subjective metrics. Even though this statement is true to a certain extent, the selection of parameters in the adaptive

filter structure mimics the differences for the observers. Therefore, we propose the use of objective quality metric Mean Square Error Image (MSEI) in (17) to be the perfect criteria in order to decide the output quality of the AUM technique.

$$Mean\ Square\ Error\ Image = \frac{1}{N \times M}\overline{e^2(n,m)} \quad (17)$$

where N is the number of rows in the error image and M is the number of columns in the error image.

The rest of this section will interpret each parameter listed in Tab. 1 and illustrate the significance on the output infrared image quality. Note that joint optimization is beyond the scope of this paper and our ultimate goal is to reduce MSEI value as minimum as possible in a cascaded manner.

i. The parameters τ_1 and τ_2 in Tab. 1 are the lower and upper limit threshold values of medium contrast level areas respectively. In [4], the input image $x(n,m)$ is split into three different contrast level areas; namely $v_i(n,m)<\tau_1$ for uniform or low contrast level areas, $\tau_1 \leq v_i(n,m)<\tau_2$ for medium contrast level areas and $v_i(n,m)\geq \tau_2$ for high contrast level areas. Also, the input image $x(n,m)$ and the variance image $v_i(n,m)$ which is calculated according to (10) are observed and it is stated in [4] that the parameters τ_1 and τ_2 are determined experimentally. In this study, our experiments show that τ_1 and τ_2 values are important while classifying the contrast areas and therefore have significant effect on sharpening the edges of the image.

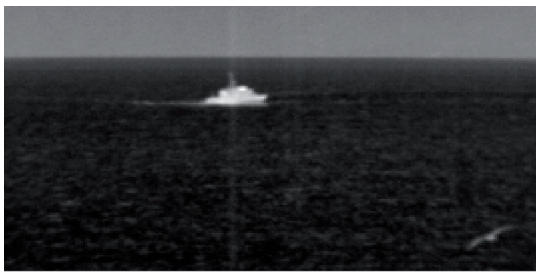

Fig. 4. The infrared input image $x(n,m)$ on which the algorithm is implemented.

In our gray scale test image (136x272 pixels) illustrated in Fig. 4, we first classified six regions of interest; namely sky, skyline, sea, ship, waves, and gull. Then we map these regions of interest to contrast areas, which is called "region classification". In terms of region classification; sea and sky belong to uniform or low contrast level areas and skyline, ship and gull belong to medium contrast level areas. Though waves in the sea belong to high contrast level areas, they are partially enhanced in order to avoid noise amplification. After region classification, the edge intensity values in the variance image $v_i(n,m)$ are used to determine τ_1 and τ_2 values. Note that in this study the idea is to sharpen the edges of the skyline, ship and gull and that the values of τ_1 and τ_2 would have been different if other regions of interest were to be sharpened. As a result; lower limit threshold value τ_1 and upper limit threshold value τ_2 for the input image in Fig. 4 are determined as 100 and 500 respectively.

ii. α_{dl} and α_{dh}, which have inequality condition as $1<\alpha_{dl}<\alpha_{dh}$ in (11), represent the coefficients to be applied to high and medium contrast level areas respectively. That is, α_{dl} and α_{dh} adjust the contrast levels by being applied to the areas which are determined by threshold parameters τ_1 and τ_2. On one hand, excessive values of α_{dh} cause saturated output image $y(n,m)$ and over artificiality occurs on high contrast level areas. On the other hand, while α_{dl} and α_{dh} have small values close to 1.0, sufficiently enhanced output image may not be obtained. As a result; α_{dl}, high contrast level enhancement coefficient and α_{dh}, medium contrast level enhancement coefficient for the input image in Fig. 4 are determined as 2 and 3 respectively.

iii. The choice of the optimum value for μ is an important step while implementing the Gauss-Newton algorithm in (15) because it determines the rate of convergence. That is; if this value is too small, it may take too many iterations to reach minimum MSEI. If however the value is too large, it will jump around MSEI value. This common problem is called "misadjustment". In order to narrow the boundary conditions of μ, the Least Mean Square (LMS) algorithm converges to the adaptive Wiener filter by using the maximum eigenvalue of the scaling vector covariance matrix, μ_{bound}. Therefore, while choosing the optimum μ, (18) should be taken into consideration:

$$0 < \mu < \frac{1}{\mu_{bound}}. \quad (18)$$

Fig. 5 shows MSEI values versus μ, which changes from 0.001 to 0.4 with 0.001 intervals. As shown in Fig. 5, for small values of μ, number of iterations is insufficient to reach the minimum MSEI value and for μ values larger than $1/\mu_{bound}$ (0.2732), the rate of convergence increases too much so that the adaptive filter jumps around the optimum MSEI value. Consequently, for the image in Fig. 4, it is wise to choose μ, the value of the convergence rate for adaptive filter, to be any number between 0.03 to 0.20. Therefore we propose the usage of (18), which proves that the boundary condition $1/\mu_{bound}$ is effective criteria to determine the optimum μ.

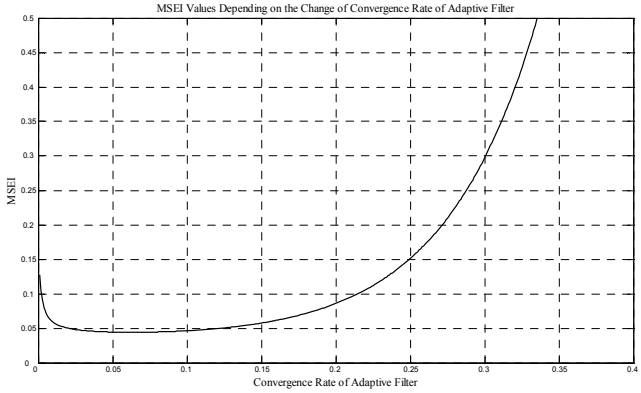

Fig. 5. MSEI values depending on the change of μ.

iv. The most important parameter that changes recursively and determines the characteristic of adaptive filter is the scaling vector $\Lambda(n,m)$. Since the initial values of the

first column of the scaling vector are determined, over artificiality occurs on the first column of the output image $y(n,m)$. However, the characteristic of the adaptive filter shows that the value of each column location in each row of the scaling vector is obtained by using the value of the same row of the previous column. So, there is an update along the rows on scaling vector values according to Gauss-Newton algorithm [14]. The objective here is to find the optimum initial values of the first column of the scaling vector $\Lambda(n,1) \mid_{n=1}^{n=N}$ for the best output image without over artificiality. We choose the initial scaling vectors as in (19),

$$\overline{\Lambda}(n,1)\Big|_{n=1}^{n=N} = \left[\lambda_x(n,1), \lambda_y(n,1)\right]^T \Big|_{n=1}^{n=N} = [0,0]^T = [0;0] \quad (19)$$

which means that the first column of the output image is the same as the first column of the input image as seen in (8). This, as expected heuristically, leads to minimum MSEI.

v. β in (16) represents positive convergence parameter and has to be less than 1. By careful examination, it is possible to observe that (16) is a linear interpolation between $\boldsymbol{R}(n,m\text{-}1)$ and $\boldsymbol{G}(n,m)\boldsymbol{G}^{\boldsymbol{T}}(n,m)$. Fig. 6 illustrates MSEI versus β which changes from 0.001 to 1 in 1,000 steps. It is evident from the figure that β should lie somewhere in between 0.4 to 0.6 for minimum MSEI. In our experiments we picked β as 0.5, which means half way between $\boldsymbol{R}(n,m\text{-}1)$ and $\boldsymbol{G}(n,m)\boldsymbol{G}^{\boldsymbol{T}}(n,m)$.

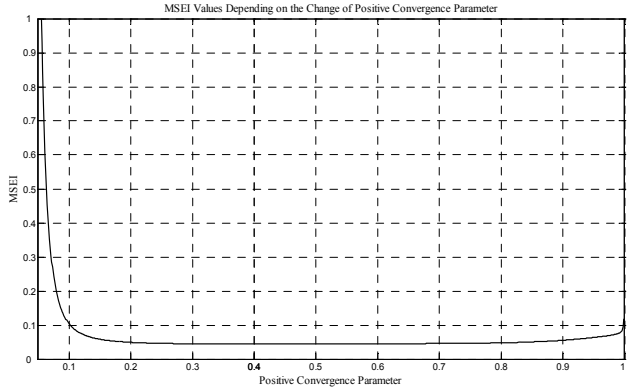

Fig. 6. MSEI values depending on the change of β.

vi. Autocorrelation matrix of the input vector to adaptive filter $\boldsymbol{G}$ and the final parameter to be investigated in Tab. 1 is $\boldsymbol{R}(n,m)$. Like the scaling vector $\boldsymbol{\Lambda}(n,m)$, the value of each column location in each row of the autocorrelation matrix is obtained by using the value of the same row of the previous column. So, the update is along the rows of the autocorrelation matrix in (16). Since β is chosen as 0.5, the update process rapidly balances initial values of the autocorrelation matrix $\boldsymbol{R}(n,1) \mid_{n=1}^{n=N}$ so that minimum MSEI is achieved. Yet, important criteria while determining $\boldsymbol{R}(n,1) \mid_{n=1}^{n=N}$ is that; the sub-matrixes have to be non-singular matrix cell arrays, that is, their determinants have to be nonzero so that inverse autocorrelation matrix could be calculated in (16). Consequently, based on the inversion problem for $\boldsymbol{R}(n,1) \mid_{n=1}^{n=N}$, initial values for the first column of the autocorrelation matrix is determined in (20) as unity for minimum complexity.

$$\boldsymbol{R}(n,1) \mid_{n=1}^{n=N} = [1,0;0,1] \quad (20)$$

4. Algorithm Implementation and Experimental Results

Tab. 2 summarizes the optimum parameters, which are carefully investigated, interpreted and selected in order to enhance the input infrared image in Fig. 4 by using the AUM technique.

Optimum Parameters Proposed for the AUM Technique
$\tau_1 = 100$
$\tau_2 = 500$
$\alpha_{dl} = 2$
$\alpha_{dh} = 3$
$\mu = 0.06$
$\Lambda(n,1)\Big\vert_{n=1}^{n=N} = [0,0]^T = [0;0]$
$\beta = 0.5$
$\boldsymbol{R}(n,1) \mid_{n=1}^{n=N} = [1,0;0,1]$

Tab. 2. Optimum parameters proposed for the AUM technique.

For the input image in Fig. 7(a), the threshold values τ_1 and τ_2 which are obtained by the distribution of the variance image in Fig. 7(b) determine which contrast level areas are to be enhanced. The proper contrast level enhancement coefficients α_{dl} and α_{dh} are shown in Fig. 7(c). According to Fig. 7(c), there is no sharpening path or enhancement for uniform areas (sky and sea), there is partial enhancement for the areas with high contrast levels (waves) and there is an eye-catching enhancement for the areas with medium contrast level (skyline, ship and gull), which the improvement is close to that of the high contrast level area.

In addition, the difference image between the desired local dynamic image $g_d(n,m)$ in Fig. 8(a) and the actual local dynamic image in Fig. 8(b), that is the error image $e(n,m)$ in Fig. 8(c), has its optimum level so that MSEI has been reduced to its minimum at 0.0442. This reference for criteria needs to be compared with the MSEI value obtained from [4] in order to appreciate the success of our work. Polesel et al. report that the parameter intervals, which have been experimentally found, are effective in providing good contrast enhancement to almost all images on which the AUM algorithm has been tested. However our experiments proved that the parameters tested within these intervals resulted with MSEI values between 0.1141 and 0.1294.

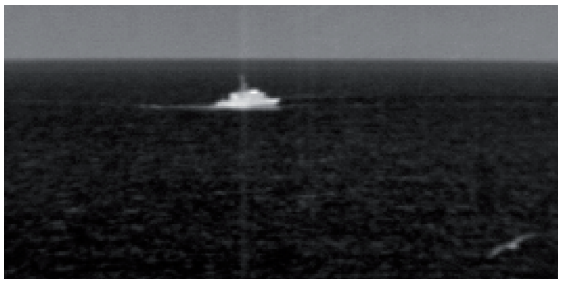

(a)

(b)

(c)

Fig. 7. (a) The input image $x(n,m)$, (b) the variance image $v_i(n,m)$, and (c) the variable gain image $\alpha(n,m)$.

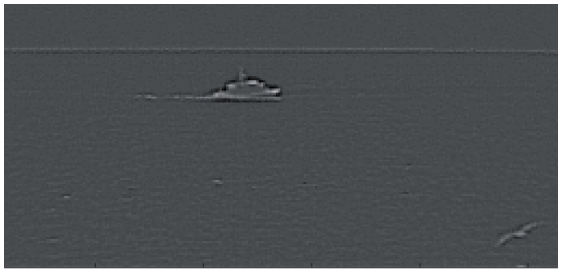

(a)

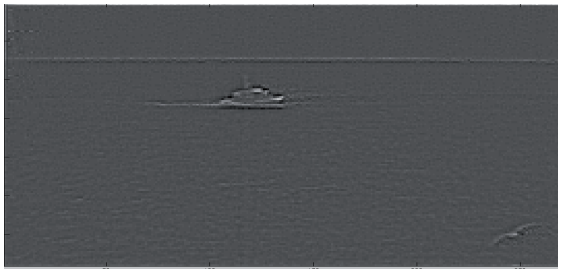

(b)

(c)

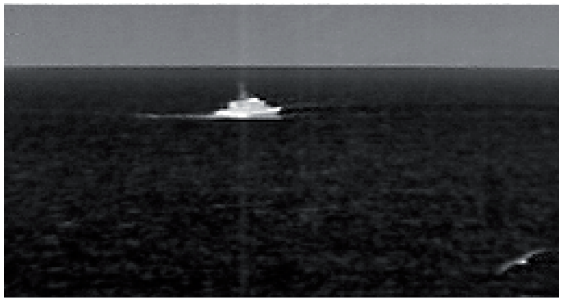

(d)

Fig. 8. (a) Desired local dynamic image $g_d(n,m)$, (b) actual local dynamic image $g_y(n,m)$, (c) error image $e(n,m)$, and (d) enhanced output image $y(n,m)$.

Consequently, the contrast and sharpness level of the ship in Fig. 9(b) and the gull in Fig. 9(d) have much better view than the levels in the original image as shown in Fig. 9(a) and Fig. 9(c).

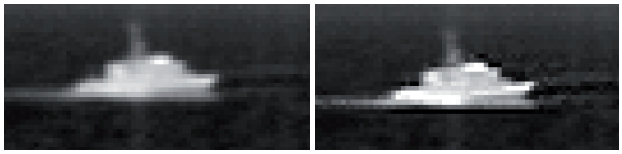

(a) (b)

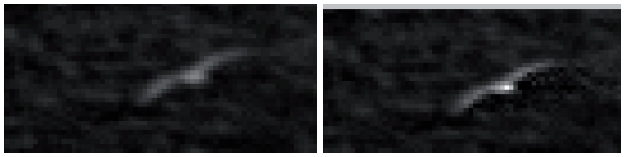

(c) (d)

Fig. 9. (a) Zoomed and (b) enhanced version of the ship; (c) zoomed and (d) enhanced version of the gull.

5. Conclusion

Images obtained from infrared devices for the purpose of surveillance, security and defense need to be enhanced in many occasions due to poor recording quality and adverse conditions. In this study, we interpreted the vital parameters and gave guidance to select optimum values for infrared images for the well-known AUM technique. The selection procedure takes many important design criteria into consideration, such as complexity reduction and per-

formance improvement on the output quality. This study is unique in the sense that the proposed criteria for optimum parameter selection are applicable to any image, in particular to infrared images. Hence, the proposed method ensures that edges of the targets in images are sharper and that the quality of contrast adjustment has its optimum level with minimum error, approximately 3 times better than that of Polesel et al. report in [4].

Acknowledgements

Onur Jane has been supported by a study grant of The Scientific and Technological Research Council of Turkey (TÜBİTAK) for his M.S. studies.

References

[1] JACKSON, J. S., COSGRIFF, R. L., BOSGESS, R. L., HAYMAN. Infrared techniques for surveillance and crime deterrence. *IEEE Transaction on Industrial Electronics and Control Instrumentation,* May 1971, vol. *IECI-18*, no. 2, p. 38 -42.

[2] HUDSON, R. D. *Infrared System Engineering*. John Wiley & Sons, Inc., 1969.

[3] KARALI, A. O., AYTAÇ, T. A comparison of different infrared image enhancement techniques for sea surface targets. In *Signal Processing and Communications Applications Conference*, SIU 9-11 April 2009, p. 765 – 768 (in Turkish).

[4] POLESEL, A., RAMPONI, G., MATHEWS, V. J. Image enhancement via adaptive unsharp masking. *IEEE Transactions on Image Processing,* March 2000, vol. 9, no. 3, p. 505 – 510.

[5] BADAMCHIZADEH, M. A., AGHAGOLZADEH, A. Comparative study of unsharp masking methods for image enhancement. In *Proceedings of the IEEE Third International Conference on Image and Graphics.* 18-20 December 2004, p. 27 to 30.

[6] GONZALEZ, R. C., WOODS R. E. *Digital Image Processing*. Prentice Hall, Upper Saddle River, NJ, 2008.

[7] LAMBRECHT, C. V. D. B. Perceptual models and architectures for video coding applications. *Ph.D. dissertation*, EPFL, Lausanne, Switzerland, 1996.

[8] WIDROW, B., STEAMS, S. D. *Adaptive Signal Processing*. Englewood Cliffs, NJ: Prentice-Hall, 1985.

[9] SINGH, M., SINGH, S. Optimizing image enhancement for screening luggage at airports. In *Proceedings of the 2005 IEEE International Conference on Computational Intelligence for Homeland Security and Personal Safety*, CIHSPS 2005, art. no. 1500627, p. 131 – 136.

[10] SINGH, M., SINGH, S., PARTRIDGE, D. A comparison of image enhancement techniques for explosive detection. In *Proceedings of the International Conference on Pattern Recognition 4*, 2004, p. 811 – 814.

[11] FERRARI, J. A., FLORES, J. L., PERCIANTE, C. D., FRINS, E. Edge enhancement and image equalization by unsharp masking using self-adaptive photochromic filters. *Applied Optics* 48 (19), 2009, p. 3570 – 3579.

[12] SINGH, M., SINGH, S., PARTRIDGE, D. A knowledge-based framework for image enhancement in aviation security. *IEEE Transactions on Systems, Man, and Cybernetics, Part B: Cybernetics 34 (6)*, 2004, p. 2354 – 2365.

[13] FRANCISCO, G. L., BILLUPS, R. B., DEHORN, T., ANSTETT, F., O'HARA, M., FISHER, D. A. Thermal imaging for law enforcement and security, post 9-11. *Proceedings of SPIE – The International Society for Optical Engineering 5071*, 2003, p. 453 – 464.

[14] HAYKIN, S. *Adaptive Filter Theory*. Prentice Hall, 2002.

About Authors

Onur JANE received the B. S. degree from Electronics Engineering Dept., Ankara University, Turkey in 2009 with summa cum laude, 4.0 GPA among both the department and the faculty. He was supported by the scholarship from Higher Education Credit General Management for his undergraduate education. He is currently an M. S. student at Electronic Engineering Dept., Ankara University. He has been supported by the Scientific and Technological Research Council of Turkey (TÜBİTAK) for his M. S. study.

Hakkı Gökhan İLK received the B. S. degree from Ankara University, Ankara, Turkey, in 1993 and the M. S. degree instrument design and application and the Ph.D. degree from the University of Manchester, Manchester, U.K., in 1994 and 1997, respectively. He is an Associate Professor with the Electronics Engineering Department, Ankara University. He is the founder of the Ankara University Speech Processing Group (AUSPG). His current research interests are signal processing and speech coding in particular. Dr. Ilk was the recipient of Ankara University's sponsorship for his postgraduate studies in the U.K. and shared Turkcell's (GSM operator) "Best Academic Award" in 2007.